# Stim1, PKCδ and RasGRP proteins set a threshold for pro-apoptotic Erk signaling during B cell development

**Andre Limnander**[1], **Philippe Depeille**[2], **Tanya S. Freedman**[1], **Jen Liou**[3], **Michael Leitges**[4,5], **Tomohiro Kurosaki**[6,7], **Jeroen P. Roose**[2], and **Arthur Weiss**[1]

[1]Department of Medicine, Howard Hughes Medical Institute, Rosalind Russell Medical Research Center for Arthritis

[2]Department of Anatomy, University of California at San Francisco, 513 Parnassus Ave, San Francisco, CA 94143

[3]Department of Physiology, University of Texas Southwestern Medical Center, 5323 Harry Hines Blvd, Dallas, Texas 75390-9040

[4]Division of Nephrology, Department of Medicine, Hannover Medical School, Hannover, Germany

[5]The Biotechnology Centre of Oslo, University of Oslo, Norway

[6]Laboratory for Lymphocyte Differentiation, WPI Immunology Frontier Research Center, Osaka University, Suita, Osaka, Japan

[7]Laboratory for Lymphocyte Differentiation, RIKEN Research Center for Allergy and Immunology, Yokohama, Kanagawa, Japan

## Abstract

Clonal deletion of autoreactive B cells is crucial to prevent autoimmunity, but the signaling mechanisms that regulate this checkpoint remain undefined. Here we characterized a previously unrecognized $Ca^{2+}$-driven Erk activation pathway, which was pro-apoptotic and biochemically distinct from DAG-induced Erk activation. This pathway required PKCδ and RasGRP proteins and depended on Stim1 concentrations, which control the magnitude of $Ca^{2+}$ entry. Developmental regulation of these proteins was associated with selective activation of the pathway in B cells prone to negative selection. This checkpoint was impaired in *PKCδ-deficient m*ice, which developed B cell autoimmunity. Conversely, Stim1 overexpression conferred a competitive disadvantage to developing B cells. These findings establish $Ca^{2+}$-dependent Erk signaling as a critical pro-apoptotic pathway that mediates B cell negative selection.

Early B cell development in the bone marrow is characterized by genetic rearrangements of the immunoglobulin locus that lead to the production of a unique B cell receptor (BCR) on the surface of each B cell. This process generates an exceptionally diverse repertoire of B cells for the recognition of potential foreign invaders. However, a sizeable portion of the initial repertoire has the ability to recognize self and these cells must be modified, silenced or eliminated to prevent later autoimmunity[1–5]. Immature bone marrow B cells initially express the BCR as membrane-bound IgM, establishing the first opportunity for the cell to recognize antigen. Antigen engagement at this stage results in upregulation of the recombination machinery and receptor editing, one way by which autoreactivity can be avoided while rescuing the cell[6]. However, as cells progress through development and continue increasing the surface abundance of IgM and IgD, they lose the ability to edit the receptor and instead become increasingly sensitive to antigen-induced apoptosis[7]. These transitional bone marrow cells thus undergo apoptosis upon antigen encounter, a second checkpoint to avoid the development of later autoimmunity. Cells that survive past this stage then leave the bone marrow and migrate to the spleen, where they undergo additional selection checkpoints before completing maturation. Once B cells reach a mature stage, they become resistant to antigen-induced apoptosis and instead mount vigorous proliferative responses to antigen. Therefore, developmental changes during B cell maturation alter signaling responses to antigen in ways that lead to different functional outcomes. The molecular mechanisms by which antigen encounter leads to editing, apoptosis or proliferation at different stages of B cell development are not well understood.

Compared to mature B cells, developing B cells display decreased diacylglycerol (DAG) production and increased amplitude and duration of $Ca^{2+}$ entry in response to antigen, particularly at low antigen concentrations[8–11]. $Ca^{2+}$ is essential for both receptor editing and antigen-induced apoptosis[7], implying that increased amplitude of $Ca^{2+}$ entry in developing B cells likely contributes to their increased sensitivity to antigen-induced apoptosis. The mechanism that drives $Ca^{2+}$ into a lymphocyte is initiated by depletion of intracellular stores: antigen receptor crosslinking leads to activation of phospholipase C-γ (PLC-γ), which converts $PtdIns(4,5)P_2$ into $Ins(1,3,4)P_3$ and DAG; $IP_3$ then binds $IP_3$ receptors on the endoplasmic reticulum (ER) membranes, leading to depletion of $Ca^{2+}$ from the ER stores. This triggers an initial increase in cytoplasmic $Ca^{2+}$ concentration, which is followed by opening of the $Ca^{2+}$ release activated $Ca^{2+}$ (CRAC) channels (or other SOC channels, such as TRP channels, depending on the cell type) at the plasma membrane. Extracellular $Ca^{2+}$ then flows into the cell following a ten-thousand-fold gradient and further prolongs the increases in intracellular $Ca^{2+}$ concentration, a process is known as store-operated $Ca^{2+}$ entry (SOCE)[12]. The mechanism that couples ER store release to opening of the plasma membrane channels has only recently been defined, in part due to the identification of Stim1 as the long-sought ER $Ca^{2+}$ sensor[13–15]. Stim1 is a transmembrane ER protein that contains a $Ca^{2+}$-binding EF hand localized in the lumen of the ER. Under resting conditions, Stim1 is $Ca^{2+}$-bound and evenly distributed through the ER membrane. Upon release of the ER $Ca^{2+}$ stores Stim1 becomes $Ca^{2+}$ unbound, clusters and moves toward the plasma membrane where it interacts with the channels[16–20], causing them to open and triggering entry of extracellular $Ca^{2+}$. Stim1 is thus essential for SOCE, but the extent to which Stim1 protein abundance influences the potential magnitude of $Ca^{2+}$ responses has not been explored.

Here we used Stim1 to establish a system for sensitization of B cells to antigen receptor-induced apoptosis. Using this system we identified and characterized a previously unrecognized $Ca^{2+}$-driven pathway involved in Erk activation. We demonstrated that Stim1 overexpression in a B cell line augmented the amplitude and duration of $Ca^{2+}$ entry and enhanced antigen receptor-induced apoptosis. By mass spectrometry we identified a $Ca^{2+}$-dependent pathway to Erk with biochemical requirements distinct from those for DAG-mediated Erk activation. Activation of this $Ca^{2+}$-dependent pathway required RasGrp and PKCδ activity, and its disruption rescued the cells from antigen receptor-induced apoptosis. Furthermore, we identified S332 on human RasGRP1 as a potential phosphorylation site that is a likely target for protein kinase Cδ and was essential for activation of this $Ca^{2+}$-Erk pathway. Stim1, PKCδ and RasGRP proteins were all differentially expressed in primary bone marrow B cells prone to negative selection and as a result, this pathway was selectively activated in these B cell subsets. *PKCδ-deficient* developing B cells failed to activate this pathway, which correlates with development of self-reactive B cells and autoimmunity in these mice[21, 22]. In contrast, developing B cells overexpressing Stim1 displayed increased negative selection at the bone marrow transitional stage, and this effect required PKCδ. Our findings demonstrate that DAG and $Ca^{2+}$ can direct Erk signaling towards different functional outcomes, thus outlining a molecular mechanism by which developmental regulation of $Ca^{2+}$- and DAG-dependent Erk pathways can determine B cell fate.

## Results

### Stim1 increases SOCE and apoptosis in DT40 B cells

Recent work has described an important role for Stim1 in store-operated $Ca^{2+}$ entry (SOCE)[13–15]. We hypothesized that Stim1 might act as the limiting factor to control the rate of CRAC channel opening and thus control induction of apoptosis. Indeed, DT40 B cells stably over-expressing eYFP-Stim1 (Supplementary Fig. 1) displayed increased amplitude and duration of SOCE relative to wild-type DT40 cells in response to either BCR stimulation, thapsigargin or cyclopiazonic acid (CPA) (Fig. 1a, Supplementary Fig. 2a). Thapsigargin and CPA trigger SOCE by inhibiting the SERCA pumps in the ER, thereby inducing passive release of $Ca^{2+}$ from the ER stores while bypassing proximal BCR signaling. Consistent with a role for $Ca^{2+}$ in antigen-induced apoptosis[8, 10], Stim1 overexpression sensitized DT40 cells to both BCR- and thapsigargin-induced apoptosis (Fig. 1b). Furthermore, chelating extracellular $Ca^{2+}$ with EGTA during either stimulation regimen rescued the cells from apoptosis. Therefore, $Ca^{2+}$-dependent pro-apoptotic signals are enhanced in Stim1-overexpressing DT40 cells.

### Increased SOCE leads to $Ca^{2+}$-dependent Erk activation

We examined the phosphotyrosine profile of Stim1-overexpressing DT40 B cells following thapsigargin stimulation for 2 and 5 minutes and observed robust and sustained tyrosine phosphorylation of a ~42 kDa band, which was only modestly detectable in thapsigargin-stimulated wild-type DT40 cells (Fig. 1c). Immunoprecipitation of this protein with a phosphotyrosine antibody (Fig. 1d), followed by mass spectrometry identified this band as Erk2. To confirm the identity of this protein, DT40 cells or Stim1-overexpressing DT40 cells were stimulated over time with thapsigargin or CPA in the presence or absence of

extracellular $Ca^{2+}$, and the phospho-Erk (pErk) responses were analyzed by flow cytometry. While $Ca^{2+}$-dependent Erk activation was modest and short-lived in wild-type DT40, it was robust and sustained in Stim1-overexpressing DT40 cells (Fig. 1e,f, Supplementary Fig. 2b). Chelation of extracellular $Ca^{2+}$ by EGTA effectively abrogated the thapsigargin- or CPA-induced pErk response, demonstrating that the robust Erk activation observed in the Stim1-overexpressing DT40 cells is due to the increased SOCE in these cells.

Antigen-induced Erk activation in lymphocytes is thought to be DAG-dependent and mostly $Ca^{2+}$-independent[23–27]. However, we hypothesized that a parallel, $Ca^{2+}$-driven pathway to Erk may become relevant in B cells when the SOCE is more intense relative to the limited DAG signals[10], and longer lasting than the DAG signal. Stim1-overexpressing DT40 cells had increased and prolonged pErk production in response to BCR stimulation with respect to wild-type DT40 cells, and the increased amplitude and duration of the response depended on extracellular $Ca^{2+}$ (Fig. 2a,b). To determine whether this pathway to Erk is predominantly triggered by $Ca^{2+}$ and less by DAG, we utilized diacylglycerol kinase $\zeta$ (DGK$\zeta$), which converts DAG to phosphatidic acid, thereby inhibiting DAG-dependent responses[28]. We transfected Stim1-overexpressing DT40 cells with DGK$\zeta$ and CD16 as a surrogate cell surface marker for transfected cells. The cells were then stimulated with either thapsigargin or a dose of anti-BCR that elicits an equivalent pErk response in the untransfected population (Fig. 2c,d). DGK$\zeta$ expression did not inhibit thapsigargin-induced $Ca^{2+}$-dependent pErk (Fig. 2c,d). In contrast, BCR crosslinking, which triggers DAG production as well as SOCE, elicited a pErk response that was partially inhibited by DGK$\zeta$. Addition of EGTA at the time of BCR crosslinking led to further inhibition of the pErk response, demonstrating that simultaneous inhibition of $Ca^{2+}$ and DAG can almost entirely ablate Erk activation in these cells. Thus, BCR stimulation can activate Erk via distinct DAG- or $Ca^{2+}$-dependent pathways and the kinetics of $Ca^{2+}$ entry and DAG production affect the relative contribution of these pathways to the overall response.

## $Ca^{2+}$-Erk signaling in bone marrow developing B cells

We next investigated whether the activation of this $Ca^{2+}$-Erk pathway that we observed in our DT40 B cell model with Stim1 expression also occurs in primary B cells. Bone marrow cells from wild-type C57BL/6 mice were stimulated with thapsigargin over time, fixed, permeabilized, stained for pErk in combination with cell surface markers and analyzed by flow cytometry. Only immature and transitional B cells, but not earlier precursors or mature recirculating B cells, displayed robust $Ca^{2+}$-dependent Erk activation (Fig. 3). $Ca^{2+}$-dependent Erk activation was less robust in splenic transitional subsets than in bone marrow immature and transitional cells (data not shown), suggesting that this pathway is more relevant in the bone marrow. Thus, B cells are altered developmentally to allow the activation of this pathway specifically in bone marrow B cell populations known to be highly sensitive to apoptosis, where an important checkpoint for the deletion of self-reactive B cells occurs.

## Loss of Stim1-overexpressing developing B cells

We next hypothesized that, similar to the effect observed in DT40 cells, increasing Stim1 in bone marrow hematopoietic progenitors might increase SOCE, enhance $Ca^{2+}$-dependent Erk

signaling and sensitize developing B cells to negative selection. To test this hypothesis, we infected bone marrow hematopoietic stem cells expressing different congenic markers with retroviruses carrying eYFP or eYFP-Stim1. These cells were used in competitive repopulation experiments and the survival of eYFP-Stim1^{+} B cells was traced throughout development relative to eYFP^{+} B cells. eYFP-Stim1^{+} cells were markedly outcompeted by eYFP^{+} cells (Fig. 4), resulting in very low numbers of eYFP-Stim1^{+} peripheral B cells. The greatest loss of Stim1+ B cells occurred in bone marrow stages that correlate with the developmental onset of $Ca^{2+}$-dependent Erk activation. Thus, increasing Stim1 expression confers a competitive disadvantage to developing B cells at the same stages that are most sensitive to thapsigargin-induced activation of Erk in unmanipulated bone marrow B lineage cells. To test whether this out-competition is due to increased negative selection, we examined the effect of Stim1 on developing MD4 transgenic B cells, which express a transgenic BCR that recognizes hen egg lysozyme (IgHEL). Hematopoietic stem cells (HSCs) from MD4 mice were infected with eYFP-Stim1 and injected into lethally irradiated wild-type recipient mice. The survival of eYFP-Stim1-transduced MD4 B cells relative to non-transduced MD4 B cells was traced throughout development. In the absence of antigen, MD4 B cells overexpressing eYFP-Stim1 competed efficiently with non-transduced cells during bone marrow development (Supplementary Fig. 3). In fact, occasionally mice demonstrated an expansion of eYFP-Stim1^{+} cells relative to non-transduced cells, an effect that is opposite to what was observed in mice with an unrestricted B cell repertoire. Therefore, restricting the BCR repertoire to IgHEL in the absence of antigen (HEL) is sufficient to rescue the competitive disadvantage of Stim1-overexpressing B cells. These findings demonstrate that Stim1 overexpression sensitizes developing B cells to negative selection.

## RasGRP-dependent $Ca^{2+}$-Erk signaling is pro-apoptotic

We next investigated the mechanism by which SOCE activates Erk to determine if a causal relationship between this pathway and apoptosis exists. Calcium increases are not generally thought to modulate the MAPK pathways leading to Erk activation. RasGrp and SOS are Ras guanine nucleotide exchange factors (RasGEFs) involved in RasGTP production upstream of Erk activation in lymphocytes[25, 29–33]. RasGrp proteins contain both DAG-binding C1 domains and $Ca^{2+}$-binding EF hands, and they have been proposed to mediate pro-apoptotic signals in B cells[34, 35]. Although DAG is important for RasGrp activity, we hypothesized that, under conditions of high SOCE, $Ca^{2+}$ could potentially trigger activation of RasGrp as well, leading to Erk activation. We first transiently transfected $Rasgrp1^{-/-}Rasgrp3^{-/-}$ or $Sos1^{-/-}Sos2^{-/-}$ DT40 cells[32] with eYFP-Stim1 and examined the ability of these cells to support Erk activation in response to thapsigargin. Thapsigargin-induced Erk activation was almost entirely abrogated in Stim1-overexpressing RasGRP-deficient cells, but was completely unaffected in SOS-deficient cells overexpressing Stim1 (Fig. 5a). We thus generated $Rasgrp1^{-/-}Rasgrp3^{-/-}$ DT40 cell lines stably overexpressing eYFP-Stim1 (Supplementary Fig. 4a), which exhibited a similar increase in SOCE to that observed in wild-type DT40 cells overexpressing Stim1 (Supplementary Fig. 4b). As expected after the transient transfection experiments, these cells displayed a near-complete loss of Erk activation in response to thapsigargin (Supplementary Fig. 4c). RasGrp deficiency rescued DT40 cells from BCR-induced apoptosis, even when Stim1 was

overexpressed (Fig. 5b). These results demonstrate that RasGrp is required to mediate Erk activation by $Ca^{2+}$ and disrupting $Ca^{2+}$-dependent activation of RasGrp and Erk is sufficient to inhibit antigen receptor-induced apoptosis.

PKC-mediated phosphorylation of RasGrp is known to be important for its activation[25, 26, 36, 37]. To determine whether $Ca^{2+}$-dependent activation of Erk requires PKC activity, we examined the effect of two different PKC inhibitors, GF-109203X and Gö6976, on thapsigargin- or anti-BCR-induced pErk. Surprisingly, the two PKC inhibitors had opposite effects. GF-109203X potently inhibited the response to thapsigargin while having a minor effect on the anti-BCR response. Gö6976 did not inhibit the response to thapsigargin, but inhibited most of the anti-BCR-induced pErk response, with the remaining pErk being $Ca^{2+}$-dependent (Fig. 5c). This result is consistent with previous studies examining the role of Gö6976 on BCR-induced pErk[36, 37]. Therefore, Gö6976 inhibits the DAG-dependent component of the BCR-mediated Erk response, but not the $Ca^{2+}$-dependent response. In contrast, GF-109203X inhibits the $Ca^{2+}$-dependent Erk response, but not the DAG-dependent response. Although both of these inhibitors are known to inhibit classical PKCs with similar potency, their ability to inhibit non-classical PKCs is different. GF-109203X, but not Gö6976, can efficiently block PKCδ activity[38], suggesting that this PKC isoform plays a critical role in $Ca^{2+}$ dependent Erk signaling.

## Ca$^{2+}$-Erk signaling requires phospho-S332 RasGRP1

The cooperation between PKC and RasGRP proteins has been well documented, but the only phosphorylation site that has thus far been identified as a target of PKCs is RasGRP1 T184, which corresponds to T133 of RasGRP3 (refs. [36, 37]). Interestingly, neither of these sites fits a PKCδ consensus target sequence. Moreover, phosphorylation of these sites is blocked by Gö6976, which does not inhibit PKCδ or $Ca^{2+}$-dependent Erk activation. Indeed, we found that T133 RasGRP3 was not phosphorylated in response to thapsigargin, and a T184A mutant RasGRP1 was largely functional in mediating Erk activation in response to SOCE (data not shown). Therefore, we hypothesized that PKCδ could potentially phosphorylate RasGRP on other sites and thereby induce activation of a functionally distinct Erk pathway. To test this hypothesis, we selected candidate sites on human RasGRP1 based on three criteria. One, putative sites possess a PKCδ consensus target sequence (S/TXXR/K); two, these sites should have a predictive phosphorylation score above 0.8 on the Netphos 2.0 server (http://www.cbs.dtu.dk/services/NetPhos/)[39]; and three, sites should be conserved across species (chicken, mouse and human) (Supplementary Fig. 5a). Five potential serine or threonine sites were identified on RasGRP1, and were individually mutated to alanine. These mutants or wild-type human RasGRP1 were transiently transfected into the Stim1-overexpressing RasGRP-deficient DT40 cells. The transfected cells were then stimulated with thapsigargin and the pErk response within the tranfected population was examined. Four of the five mutant proteins were able to support $Ca^{2+}$-dependent Erk activation (Supplementary Fig. 5b). However, RasGRP1 S332A was completely deficient in activation of this pathway, resulting in comparably low pErk activation as observed in the parental RasGRP-deficient cells (Fig. 6a). The S332A mutant RasGRP1 was expressed in an amount comparable to that observed in wild-type RasGRP1 transfectants (Supplementary Fig. 6), ensuring that this effect was not due to lack of

expression or decreased stability of the protein. We then examined the ability of this mutant to support DAG-mediated Erk activation.

Remarkably, when the cells were stimulated with anti-BCR in the presence of EGTA, the S332A mutant RasGRP1 was able to support activation of Erk, albeit less than wild-type RasGRP1 (Fig. 6b). This result demonstrates that the S332A mutation does not result in a completely inactive nucleotide exchange factor, but rather represents a crucial site that modulates the selective responsiveness of the exchange factor to $Ca^{2+}$-induced signals. To further address whether S332 phosphorylation is involved in $Ca^{2+}$-induced Erk activation, we generated a phosphomimetic S332D RasGrp1 mutant. The S332D mutant was fully functional and induced Erk activation in response to $Ca^{2+}$ to the same extent as wild-type RasGRP1 (Fig. 6c). The same was true of the DAG-dependent BCR response, as measured by stimulation with anti-BCR in the presence of EGTA (Fig. 6d). These results demonstrate that phosphorylation of S332 is absolutely required for $Ca^{2+}$-dependent, but not for the DAG-dependent BCR-induced Erk activation. Interestingly, cells expressing the phosphomimetic mutant RasGrp1 did not exhibit constitutive Erk activation in unstimulated cells, suggesting that although phosphorylation of S332 is required, it may not be sufficient to constitutively activate the pathway.

Given the robust impact of the S332A mutation on the ability of RasGRP1 to mediate $Ca^{2+}$-dependent Erk activation, we performed homology modeling using the ModWeb server[40] and the template mouse RasGRF1 (pdb 2IJE)[41] to gain insight into the possible role this site could play in the regulation of RasGRP1 activity (Fig. 6e). Interestingly, this model predicts that S332 lies on the "flap2" region of the CDC25 domain, where a phosphorylation event could affect Ras binding and/or the positioning of the catalytic helical hairpin.

## Developmental regulation of Stim1, RasGRP and PKCδ

To determine whether developmental regulation of protein expression might play a role in the selective activation of this pathway during negative selection, we sorted bone marrow B cell subsets and examined the expression of Stim1, PKCδ and RasGRP proteins. Consistent with a role for this pathway in antigen-induced apoptosis, expression of RasGRP1, RasGRP3, PKCδ and Stim1 were all increased at the bone marrow transitional stage, where negative selection occurs (Supplementary Fig. 7). This stage was also where higher amplitude and faster kinetics of thapsigargin-induced SOCE (Supplementary Fig. 8) and maximal thapsigargin-induced pErk responses occurred (Fig. 3). Expression of RasGRP1, PKCδ and Stim1 was then downregulated in mature B cells, while RasGRP3 abundance increased further in mature B cells. The pattern of PKCδ expression was consistent with previously published results examining expression of the *LacZ* gene that was introduced into the *Prkcd* locus in the *Prkcd*$^{-/-}$ mice[21].

Likewise, the increase in RasGRP1 and PKCδ protein in bone marrow transitional B cells was also consistent with robust changes in mRNA abundance reported in the Immunological Genome Research Project (IMMGEN) website (http://www.immgen.org/databrowser/index.html). These results suggest that transient increases in RasGRP1, PKCδ and Stim1 could contribute to the preferential activation of the $Ca^{2+}$-Erk pathway in developing B cells, and that downregulation of these proteins in mature B cells may contribute to the loss

of sensitivity to antigen-induced apoptosis. By contrast, the expression pattern of RasGRP3 suggests this protein may also be involved in DAG-mediated Erk signaling in mature B cells.

## Ca²⁺-Erk signaling in developing B cells requires PKCδ

The notion that PKCδ may be required for $Ca^{2+}$-dependent Erk activation during B cell negative selection is intriguing, given the phenotype of *Prkcd*$^{-/-}$ mice[21, 22]. These mice display two-fold and seven-fold increases in B cell numbers in the spleen and lymph nodes, respectively. In these mice, self-reactive B cells develop, terminally differentiate, but fail to become anergized. The *Prkcd*$^{-/-}$ mice develop anti-nuclear antibodies and die prematurely at 9–12 months of age due to autoimmune disease. Previous studies on these mice have focused on defects in peripheral B cell homeostasis that contribute to the phenotype[42]. However, based on the developmental regulation of $Ca^{2+}$-dependent Erk activation, we hypothesized that the phenotype of the *Prkcd*$^{-/-}$ mice may be at least partly due to an inability to activate the $Ca^{2+}$-regulated Erk pathway during B cell negative selection. We performed competitive repopulation experiments, where *Prkcd*$^{-/-}$ and wild-type bone marrow cells were mixed at a 1:1 ratio and injected into lethally irradiated mice. As expected, the *Prkcd*$^{-/-}$ B cells out-competed the wild-type cells (Fig. 7a). Interestingly, the earliest developmental stage where this effect was observed coincided with the bone marrow stage where $Ca^{2+}$-dependent Erk activation occurred and where increases in Stim1 expression enhanced negative selection, whereas it was not observed in the developmental stages prior to antigen receptor expression. This observation suggests that the competitive advantage of *Prkcd*$^{-/-}$ B cells relates to alteration of developmental stage-specific signals.

We then hypothesized that the competitive advantage of *Prkcd*$^{-/-}$ bone marrow transitional B cells might relate to a loss of pro-apoptotic $Ca^{2+}$-Erk signaling at this developmental stage. Thapsigargin-induced SOCE was comparable or slightly higher in *Prkcd*$^{-/-}$ cells than in wild-type cells (Supplementary Fig. 8). However, $Ca^{2+}$-dependent Erk activation was markedly impaired in *Prkcd*$^{-/-}$ bone marrow developing B cells (Fig. 7b,c). The cell populations analyzed contain comparable numbers of newly generated B cells in both genotypes, as revealed by the rates of BrdU incorporation (Supplementary Fig. 9). Therefore, loss of $Ca^{2+}$-dependent Erk signaling in transitional *Prkcd*$^{-/-}$ bone marrow B cells may increase survival of self-reactive B cells that would otherwise undergo apoptosis, thus setting the stage for the previously described autoimmune phenotype (Supplementary Fig. 10a,b). By contrast, enhancing activation of this pathway by increasing Stim1 concentrations (Fig. 4) may lead to increased activation of this pathway, leading to increased negative selection (Supplementary Fig. 10c).

## PKCδ deficiency rescues Stim1-overexpressing B cells

Lastly, we sought to examine whether the Stim1-mediated sensitization of B cells to negative selection in the bone marrow (Fig. 4) depends on this SOCE-PKCδ-RasGRP-Erk pathway. We infected wild-type or *Prkcd*$^{-/-}$ HSCs with eYFP-Stim1, then mixed at a 1:1 ratio with eYFP-infected wild-type cells, and injected the mixed population into lethally irradiated recipients. The mice were analyzed 6–8 weeks post-injection, and the eYFP-Stim1:eYFP ratio was determined throughout the bone marrow developing B cell

populations. As previously shown in Fig. 4, wild-type Stim1-overexpressing B cells displayed a competitive disadvantage at the immature and transitional stages in the bone marrow (Fig. 8, black bars). In contrast, Stim1-overexpressing *Prkcd*$^{-/-}$ B cells displayed a competitive advantage over wild-type cells expressing eYFP alone (Fig. 8, gray bars), indicating that PKCδ is required for Stim1 to sensitize B cells to negative selection at this developmental stage. Interestingly, the composition of the mature recirculating B cell population in these mice was highly variable (data not shown), perhaps indicative of a more complex epistatic relationship between PKCδ and Stim1 in peripheral B cell homeostasis. Nevertheless, these results further support a model where Ca$^{2+}$-dependent Erk signaling, mediated by PKCδ and RasGRP proteins, sets a threshold for negative selection in the bone marrow (Supplementary Fig. 10).

## Discussion

Our data reveal the existence of a Ca$^{2+}$-dependent pro-apoptotic pathway to Erk activation, which mediates a critical checkpoint during B cell development. We therefore propose a model where Ca$^{2+}$ and DAG can direct Erk to distinct functional outcomes during B cell development. Because DAG and IP$_3$ are produced at equal molar concentrations downstream of PLCγ-mediated hydrolysis of PtdIns(4,5)P$_2$, DAG production is inextricably linked to Ins(1,3,4)P$_3$ -induced SOCE. However, the amplitude and duration of DAG production and SOCE largely depends on proteins that amplify or negatively regulate these second messengers. For example, higher amounts of Stim1 protein (which we observed in bone marrow transitional cells) may contribute to amplify SOCE. By contrast, lower DAG production, which have been previously reported in immature B cells[10], may be the result of rapid DAG turn-over mediated by DAG kinases, DAG acyltransferases or DAG lipases, all of which metabolize DAG into different products. Data from the IMMGEN website show that mRNA abundance for some of these proteins, such as DGKδ, DGKτ, DGKη, DGLβ or DGAT2L6, change during B cell development in ways that may affect DAG metabolism. In addition, we have found that considerable changes in expression of proteins that mediate the activation of Erk pathways during development also contribute to their amplification, as demonstrated by the robust increases of RasGRP1 and PKCδ expression in transitional bone marrow B cells relative to other B cell subsets. These changes in expression are likely critical to setting the appropriate threshold of antigenic signal strength that results in negative selection.

The involvement of PKCδ in this pro-apoptotic Erk pathway is intriguing and was not expected. PKCδ has been implicated in apoptosis of multiple cell types[43, 44], but the potential involvement of pro-apoptotic Ras–Erk signaling as an effector pathway downstream of PKCδ has not been explored. Therefore, our data implicating PKCδ in antigen-induced pro-apoptotic Ras–Erk signaling establish a new paradigm that could be tested in other systems where PKCδ is important to mediate apoptosis. It has been clearly demonstrated that *Prkcd*$^{-/-}$ mice display a defect in peripheral B cell homeostasis which increases the lifespan of B cells and is independent of selection events[21, 42]. However, our data involving PKCδ in pro-apoptotic Erk signaling during negative selection now suggest that loss of PKCδ may also result in previously unrecognized alterations to the B cell repertoire that contribute to the disease pathology of the mice. Interestingly, PKCδ has been

reported to be dispensable in a transgenic model of negative selection mediated by expression of membrane-bound hen egg lysozyme (HEL) in MD4 mice, which express IgHEL-specific B cells[21], implying that this may not be the only pathway mediating B cell negative selection. However, membrane-bound HEL in that model provides an exceedingly strong antigenic stimulus, in particular to a high affinity BCR transgene, which may override mechanisms that establish selection thresholds for many antigens in normal cells, thus leading to B cell deletion at the earliest bone marrow immature stage[45, 46]. Because the onset of PKCδ-mediated, $Ca^{2+}$-dependent Erk activation occurs in $IgM^{hi}IgD^{int}$ bone marrow transitional B cells, it is not surprising that the mHEL system does not reveal the role of PKCδ in negative selection.

Ras and Erk activation have been intensively studied in lymphocytes, and have mostly been thought of as DAG-dependent and $Ca^{2+}$-independent. Our findings demonstrate that more than one pathway leading to Erk activation exists in B lymphocytes, and here we show that a $Ca^{2+}$-dependent Erk activation pathway directs the functional outcome of the stimulus towards an apoptotic fate in developing B cells. Because RasGRP1 is prominently and exclusively expressed in B cell subsets where this pathway is active, we focused on defining the biochemical mechanisms by which $Ca^{2+}$ may influence its function. We have thus identified S332 on RasGRP1 as a potential phosphorylation site that is a likely PKCδ target and which was clearly required for $Ca^{2+}$-dependent Erk activation. Unexpectedly, this site is located within the CDC25 domain of RasGRP1, the domain that actually mediates the interaction with Ras and consequently the nucleotide exchange function of the protein. Because of this, a phosphorylation event that preserves nucleotide exchange function (as is the case with S332) is unlikely to trigger structural reorganization of the protein. Based on homology modeling with the CDC25 of RasGRF1[41, 47], we predict that this site lies in the "flap2" region of the CDC25 domain, which may have a role in positioning the catalytic helical hairpin of the exchange factor for catalysis. This residue is strikingly close to the Ras binding site and, because of the increase in negative charge associated with phosphorylation, electrostatic interactions may influence the choice of Ras isoform that interacts with RasGRP1. This interesting idea that may help explain how distinct Ras protein signaling pathways that rely on Erk achieve specificity.

The Ras–Erk pathway is remarkably promiscuous in terms of potential substrates, and it has been suggested that specificity is achieved through compartmentalization mediated by scaffolds that constrain active Erk to signaling complexes where they can be activated by appropriate stimuli and simultaneously gain access to appropriate substrates[48–50]. As mentioned above, phosphorylation of S332 on RasGRP1 could potentially contribute to such specificity. However, although it is clear that phosphorylation of S332 RasGRP1 is essential for SOCE to induce activation of this Erk pathway, the results with the phosphomimetic mutant suggest that this event is also not sufficient to activate it, and that other $Ca^{2+}$-dependent events may be required. Because PKCδ is not thought to bind $Ca^{2+}$ directly, it is possible that $Ca^{2+}$ binding to RasGRP via the EF hands contributes to promote RasGRP activity, possibly by facilitating the interaction with PKCδ. Moreover, at this point we cannot exclude the possibility that other $Ca^{2+}$-responsive proteins may play a role within this signaling complex, perhaps by further modifying PKCδ and/or RasGRP and potentiating their activity. Concentration gradients of DAG and $Ca^{2+}$ are also known to affect

localization of signaling proteins, and may contribute to directing distinct Erk pathways to unique compartments within the cell. Interestingly, recent results in thymocytes have implicated differential localization of MAPK signals in setting the thresholds of positive and negative selection[51]. These findings, combined with our data, suggest that $Ca^{2+}$ and DAG may control selection by directing the assembly and localization of different MAPK signaling complexes.

## Methods

### Cell culture

φNX and 3T3 cells were maintained in DMEM (CellGro) supplemented with 10% FBS, Penicillin, Streptomycin, and L-Glutamine (complete media). DT40 cells were maintained in complete RPMI (Gibco) with additional 1% chicken serum and β-mercaptoethanol (Gibco). *Rasgrp1*$^{-/-}$*Rasgrp3*$^{-/-}$ and *Sos1*$^{-/-}$*Sos2*$^{-/-}$ DT40 cells were previously described[32].

### Mice

*Prkcd*$^{-/-}$ mice were previously described[21]. C57BL/6 and BoyJ mice were purchased from Jackson Laboratory. Mouse experiments were reviewed and approved by the Institutional Animal Care and Use Committee (IACUC) at UCSF.

### Antibodies, reagents and inhibitors

Antibodies to murine IgD (11–26), IgM (II/41), B220 (RA3-6B2), CD45.1 (A20), CD45.2 (104), CD43 (S7), CD21 (7G6), CD23 (B3B4), CD93 (AA4.1) conjugated to FITC, PE, PerCP-Cy5.5, PE-Cy7, Pacific Blue, allophycocyanin, or Alexa Fluor 647 were obtained from eBioscience, Biolegend or BD Biosciences. Annexin V conjugated to PE or Pacific Blue were from BD Biosciences and Biolegend. DAPI was from Roche. FITC-conjugated F(ab) monomeric fragment and goat anti-rabbit IgG Abs conjugated to allophycocyanin were obtained from Jackson ImmunoResearch Laboratories. CD16 antibody conjugated to PE or allophycocyanin was obtained from Caltag Laboratories. Phospho-Erk (#197G2), total Erk (#9102), RasGRP3 (C33A3) and PKCδ (#2058) antibodies were obtained from Cell Signaling, RasGRP1 (m199) antibody from Santa Cruz and Stim1 (#610954) antibody from BD. Thapsigargin, Gö6976 and GF-109203X were obtained from Calbiochem. IL-3, IL-6 and stem cell factor were obtained from Peprotech. Lipofectamine 2000 was from Invitrogen. BrdU labeling was performed per manufacturer's instructions using the BrdU labeling kit from BD.

### Plasmids, retroviruses, transfections and infections

The pDS SP-YFP-Stim1and pEF- Flag-hDGKζ plasmids were previously described[13][28]. For DT40 transfections, cells were washed and resuspended at $6.6 \times 10^7$ cells/ml in serum-free RPMI. The cells were electroporated at 300V for 10 msec using a square-wave electroporator (BTX ECM 800), rested for 15 min, and plated in complete DT40 media without antibiotics.

Retroviral eYFP and eYFP-Stim1 constructs were generated by subcloning these genes into an MSCV-IThy1.1 vector by blunt-end ligation. A peYFP-N1 plasmid (Clontech) was

digested with NheI and Not1, the eYFP-Stim1 plasmid with NheI and BglII, and the vector with NotI. All digested DNA fragments were blunted and ligated using a blunt-end ligation kit (Takara). Retroviruses were generated by Lipofectamine 2000 cotransfection (carried out per manufacturer's instructions) of these constructs with pCL-Eco into φNX-Eco cells. Supernatants were collected 24 and 48 h post-transfections. 3T3 cells were infected with the viral supernatants and viral titers were determined based on percent eYFP-expressing cells by FACS. Only supernatants with titers higher than $10^6$ particles/ml (assuming every virus infects a cell and a cell does not divide following infection) were used for infections of primary bone marrow cells. For infections, MACS-purified hematopoietic stem cells were incubated overnight in complete DMEM supplemented with 15% FCS, 20 ng/ml IL-3, 10 ng/ml IL-6 and 100 ng/ml SCF. On day 2, the cells were resuspended in viral supernatant supplemented with 8 μg/ml polybrene, 15% FCS, 20 ng/ml IL-3, 10 ng/ml IL-6 and 100 ng/ml SCF, and plated on 6-well plates. Cells were centrifuged for 2 h at 30 °C and incubated overnight at 37 °C. The infection was repeated on day 3, and injections were carried out on day 4 (see bone marrow reconstitutions section).

### Immunoprecipitation, immunoblotting and mass spectrometry analysis

DT40 cells were lysed in 1% NP40 buffer supplemented with protease and phosphatase inhibitors at $10^7$ cells/ml. Sorted bone marrow cells were lysed at $5 \times 10^6$ cells/ml. Immunoblotting and immunoprecipitations were performed essentially as described before[25]. For mass spectrometry analysis, 4G10 immunoprecipitates were resolved by SDS-PAGE, stained with colloidal blue (Invitrogen), and the band of interest was excised and digested with trypsin. Tryptic digests were submitted to the Biomolecular Resource Center Mass Spectrometry Facility at UCSF for nano-electrospray LC/MS/MS and peptide mass fingerprint analyses.

### Intracellular Ca$^{2+}$ measurements

Cells were loaded with Indo-1 (Molecular Probes) per manufacturer's instructions. Ca$^{2+}$-free and Ca$^{2+}$-bound emissions were measured during stimulation of the cells using a fluorimeter (Hitachi F-4500 or Molecular Devices Flexstation3). Primary cells were analyzed by multicolor flow cytometry as previously described[9].

### Intracellular pErk staining

Primary bone marrow cells were harvested on pre-warmed serum-free DMEM supplemented with HEPES pH 7.2, non-essential aminoacids, sodium pyruvate, β-Mercaptoethanol, penicillin, streptomycin and L-Glutamine. Cells were rested at 37 °C for 1 h in media containing a 1:5000 dilution of non-stimulatory FITC- labeled F(ab) monomeric fragment, then stimulated with thapsigargin for the indicated times, fixed with pre-warmed cytofix (BD) for 15 min, washed twice with flow cytometry buffer, and permeabilized in ice-cold methanol for 45 min on ice. Cells were then washed three times, incubated for 45 minutes in flow cytometry buffer containing pErk (Cell Signaling) antibody with 4% mouse serum, washed twice and stained with an anti-rabbit secondary antibody, along with antibodies against B220 and IgD. The cells were then analyzed by flow cytometry (as detailed in Supplementary methods). The same protocol was followed for DT40 cells, except stimulation was performed in serum- free RPMI supplemented with β-

mercaptoethanol, and the staining was only for pErk (except for transiently transfected cells, which were costained for CD16).

## Bone marrow reconstitutions

Bone marrow cells from donor mice as indicated for each experiment were harvested, stem cells were purified using a MACS stem cell purification kit (Miltenyi Biotech) and cultured overnight in complete media containing IL-3, IL-6 and SCF. The cells were then infected with retroviruses carrying eYFP or eYFP-Stim1. The cells were counted, mixed at a 1:1 ratio, mixed with a 1:1 mixture of uninfected carrier bone marrow of the same genotype and injected into irradiated CD45.2$^{+/+}$ host recipients. Bone marrow, spleen and lymph nodes from host recipients were harvested 8–10 weeks post-injection and analyzed by flow cytometry.

## Flow Cytometry

Single cell suspensions were prepared from bone marrow, lymph nodes (LN) and spleens. Fc receptors were blocked with rat anti-CD16/32 (clone 2.4G2; BD Biosciences). $1–3 \times 10^6$ cells were stained with the indicated Abs and analyzed on a FACSCalibur (BD Biosciences), CyAN ADP (Beckman Coulter), Gallios (Beckman Coulter) or LSRII (BD Biosciences) flow cytometry system. Forward and side scatter exclusion was generally used to identify live cells. For analysis of bone marrow chimeras, costaining with DAPI was used to exclude dying cells as well. Data analysis was performed using FlowJo (version 8.8.4) software (Tree Star). Cell sorting was performed using a MoFlo system.

## Statistical analysis

Error bars were calculated as standard error of the mean with n ranging between 3 and 11 as indicated in each figure legend. P values for comparisons across B cell subsets were calculated using a paired T test, where values for each individual mouse were paired. P values for comparisons across different mice (of different genotype) were calculated using unpaired T test.

# Supplementary Material

Refer to Web version on PubMed Central for supplementary material.

# Acknowledgments

# References

1. Gay D, Saunders T, Camper S, Weigert M. Receptor editing: an approach by autoreactive B cells to escape tolerance. J Exp Med. 1993; 177:999–1008. [PubMed: 8459227]

2. Goodnow CC, et al. Altered immunoglobulin expression and functional silencing of self-reactive B lymphocytes in transgenic mice. Nature. 1988; 334:676–682. [PubMed: 3261841]

3. Nemazee DA, Burki K. Clonal deletion of B lymphocytes in a transgenic mouse bearing anti-MHC class I antibody genes. Nature. 1989; 337:562–566. [PubMed: 2783762]

4. Tiegs SL, Russell DM, Nemazee D. Receptor editing in self-reactive bone marrow B cells. J Exp Med. 1993; 177:1009–1020. [PubMed: 8459201]

5. Wardemann H, et al. Predominant autoantibody production by early human B cell precursors. Science (New York, N Y. 2003; 301:1374–1377.

6. Hertz M, Nemazee D. BCR ligation induces receptor editing in IgM+IgD- bone marrow B cells in vitro. Immunity. 1997; 6:429–436. [PubMed: 9133422]

7. Melamed D, Benschop RJ, Cambier JC, Nemazee D. Developmental regulation of B lymphocyte immune tolerance compartmentalizes clonal selection from receptor selection. Cell. 1998; 92:173–182. [PubMed: 9458042]

8. Benschop RJ, Brandl E, Chan AC, Cambier JC. Unique signaling properties of B cell antigen receptor in mature and immature B cells: implications for tolerance and activation. J Immunol. 2001; 167:4172–4179. [PubMed: 11591737]

9. Gross AJ, Lyandres JR, Panigrahi AK, Prak ET, DeFranco AL. Developmental acquisition of the Lyn-CD22-SHP-1 inhibitory pathway promotes B cell tolerance. J Immunol. 2009; 182:5382–5392. [PubMed: 19380785]

10. Hoek KL, et al. Transitional B cell fate is associated with developmental stage-specific regulation of diacylglycerol and calcium signaling upon B cell receptor engagement. J Immunol. 2006; 177:5405–5413. [PubMed: 17015726]

11. King LB, Norvell A, Monroe JG. Antigen receptor-induced signal transduction imbalances associated with the negative selection of immature B cells. J Immunol. 1999; 162:2655–2662. [PubMed: 10072508]

12. Parekh AB, Putney JW Jr. Store-operated calcium channels. Physiol Rev. 2005; 85:757–810. [PubMed: 15788710]

13. Liou J, et al. STIM is a Ca2+ sensor essential for Ca2+-store-depletion-triggered Ca2+ influx. Curr Biol. 2005; 15:1235–1241. [PubMed: 16005298]

14. Roos J, et al. STIM1, an essential and conserved component of store-operated Ca2+ channel function. J Cell Biol. 2005; 169:435–445. [PubMed: 15866891]

15. Zhang SL, et al. STIM1 is a Ca2+ sensor that activates CRAC channels and migrates from the Ca2+ store to the plasma membrane. Nature. 2005; 437:902–905. [PubMed: 16208375]

16. Liou J, Fivaz M, Inoue T, Meyer T. Live-cell imaging reveals sequential oligomerization and local plasma membrane targeting of stromal interaction molecule 1 after Ca2+ store depletion. Proc Natl Acad Sci USA. 2007; 104:9301–9306. [PubMed: 17517596]

17. Luik RM, Wu MM, Buchanan J, Lewis RS. The elementary unit of store-operated Ca2+ entry: local activation of CRAC channels by STIM1 at ER-plasma membrane junctions. J Cell Biol. 2006; 174:815–825. [PubMed: 16966423]

18. Park CY, et al. STIM1 clusters and activates CRAC channels via direct binding of a cytosolic domain to Orai1. Cell. 2009; 136:876–890. [PubMed: 19249086]

19. Spassova MA, et al. STIM1 has a plasma membrane role in the activation of store-operated Ca(2+) channels. Proc Natl Acad Sci USA. 2006; 103:4040–4045. [PubMed: 16537481]

20. Wu MM, Buchanan J, Luik RM, Lewis RS. Ca2+ store depletion causes STIM1 to accumulate in ER regions closely associated with the plasma membrane. J Cell Biol. 2006; 174:803–813. [PubMed: 16966422]

21. Mecklenbrauker I, Saijo K, Zheng NY, Leitges M, Tarakhovsky A. Protein kinase Cdelta controls self-antigen-induced B-cell tolerance. Nature. 2002; 416:860–865. [PubMed: 11976686]

22. Miyamoto A, et al. Increased proliferation of B cells and auto-immunity in mice lacking protein kinase Cdelta. Nature. 2002; 416:865–869. [PubMed: 11976687]

23. Dower NA, et al. RasGRP is essential for mouse thymocyte differentiation and TCR signaling. Nat Immunol. 2000; 1:317–321. [PubMed: 11017103]

24. Roose J, Weiss A. T cells: getting a GRP on Ras. Nat Immunol. 2000; 1:275–276. [PubMed: 11017094]

25. Roose JP, Mollenauer M, Gupta VA, Stone J, Weiss A. A diacylglycerol-protein kinase C-RasGRP1 pathway directs Ras activation upon antigen receptor stimulation of T cells. Mol Cell Biol. 2005; 25:4426–4441. [PubMed: 15899849]

26. Teixeira C, Stang SL, Zheng Y, Beswick NS, Stone JC. Integration of DAG signaling systems mediated by PKC-dependent phosphorylation of RasGRP3. Blood. 2003; 102:1414–1420. [PubMed: 12730099]

27. Downward J, Graves JD, Warne PH, Rayter S, Cantrell DA. Stimulation of p21ras upon T-cell activation. Nature. 1990; 346:719–723. [PubMed: 2201921]

28. Zhong XP, et al. Enhanced T cell responses due to diacylglycerol kinase zeta deficiency. Nat Immunol. 2003; 4:882–890. [PubMed: 12883552]

29. Das J, et al. Digital signaling and hysteresis characterize ras activation in lymphoid cells. Cell. 2009; 136:337–351. [PubMed: 19167334]

30. Ebinu JO, et al. RasGRP, a Ras guanyl nucleotide- releasing protein with calcium- and diacylglycerol-binding motifs. Science (New York, N Y. 1998; 280:1082–1086.

31. Ebinu JO, et al. RasGRP links T-cell receptor signaling to Ras. Blood. 2000; 95:3199–3203. [PubMed: 10807788]

32. Oh-hora M, Johmura S, Hashimoto A, Hikida M, Kurosaki T. Requirement for Ras guanine nucleotide releasing protein 3 in coupling phospholipase C-gamma2 to Ras in B cell receptor signaling. J Exp Med. 2003; 198:1841–1851. [PubMed: 14676298]

33. Roose JP, Mollenauer M, Ho M, Kurosaki T, Weiss A. Unusual interplay of two types of Ras activators, RasGRP and SOS, establishes sensitive and robust Ras activation in lymphocytes. Mol Cell Biol. 2007; 27:2732–2745. [PubMed: 17283063]

34. Guilbault B, Kay RJ. RasGRP1 sensitizes an immature B cell line to antigen receptor-induced apoptosis. J Biol Chem. 2004; 279:19523–19530. [PubMed: 14970203]

35. Stang SL, et al. A proapoptotic signaling pathway involving RasGRP, Erk, and Bim in B cells. Exp Hematol. 2009; 37:122–134. [PubMed: 19100522]

36. Aiba Y, et al. Activation of RasGRP3 by phosphorylation of Thr-133 is required for B cell receptor-mediated Ras activation. Proc Natl Acad Sci USA. 2004; 101:16612–16617. [PubMed: 15545601]

37. Zheng Y, et al. Phosphorylation of RasGRP3 on threonine 133 provides a mechanistic link between PKC and Ras signaling systems in B cells. Blood. 2005; 105:3648–3654. [PubMed: 15657177]

38. Martiny-Baron G, et al. Selective inhibition of protein kinase C isozymes by the indolocarbazole Go 6976. J Biol Chem. 1993; 268:9194–9197. [PubMed: 8486620]

39. Blom N, Gammeltoft S, Brunak S. Sequence and structure-based prediction of eukaryotic protein phosphorylation sites. J Mol Biol. 1999; 294:1351–1362. [PubMed: 10600390]

40. Eswar N, et al. Tools for comparative protein structure modeling and analysis. Nucleic acids res. 2003; 31:3375–3380. [PubMed: 12824331]

41. Freedman TS, et al. A Ras-induced conformational switch in the Ras activator Son of sevenless. Proc Natl Acad Sci USA. 2006; 103:16692–16697. [PubMed: 17075039]

42. Mecklenbrauker I, Kalled SL, Leitges M, Mackay F, Tarakhovsky A. Regulation of B-cell survival by BAFF-dependent PKCdelta-mediated nuclear signalling. Nature. 2004; 431:456–461. [PubMed: 15361883]

43. Steinberg SF. Distinctive activation mechanisms and functions for protein kinase Cdelta. Biochem J. 2004; 384:449–459. [PubMed: 15491280]

44. Yoshida K. PKCdelta signaling: mechanisms of DNA damage response and apoptosis. Cell Signal. 2007; 19:892–901. [PubMed: 17336499]

45. Hartley SB, et al. Elimination of self-reactive B lymphocytes proceeds in two stages: arrested development and cell death. Cell. 1993; 72:325–335. [PubMed: 8431943]

46. Hartley SB, et al. Elimination from peripheral lymphoid tissues of self-reactive B lymphocytes recognizing membrane-bound antigens. Nature. 1991; 353:765–769. [PubMed: 1944535]

47. Freedman TS, et al. Differences in flexibility underlie functional differences in the Ras activators son of sevenless and Ras guanine nucleotide releasing factor 1. Structure. 2009; 17:41–53. [PubMed: 19141281]

48. Kolch W. Coordinating ERK/MAPK signalling through scaffolds and inhibitors. Nat Rev Mol Cell Biol. 2005; 6:827–837. [PubMed: 16227978]

49. Murphy LO, Blenis J. MAPK signal specificity: the right place at the right time. Trends Biochem Sci. 2006; 31:268–275. [PubMed: 16603362]

50. Philips MR. Compartmentalized signalling of Ras. Biochem Soc Trans. 2005; 33:657–661. [PubMed: 16042567]

51. Daniels MA, et al. Thymic selection threshold defined by compartmentalization of Ras/MAPK signalling. Nature. 2006; 444:724–729. [PubMed: 17086201]
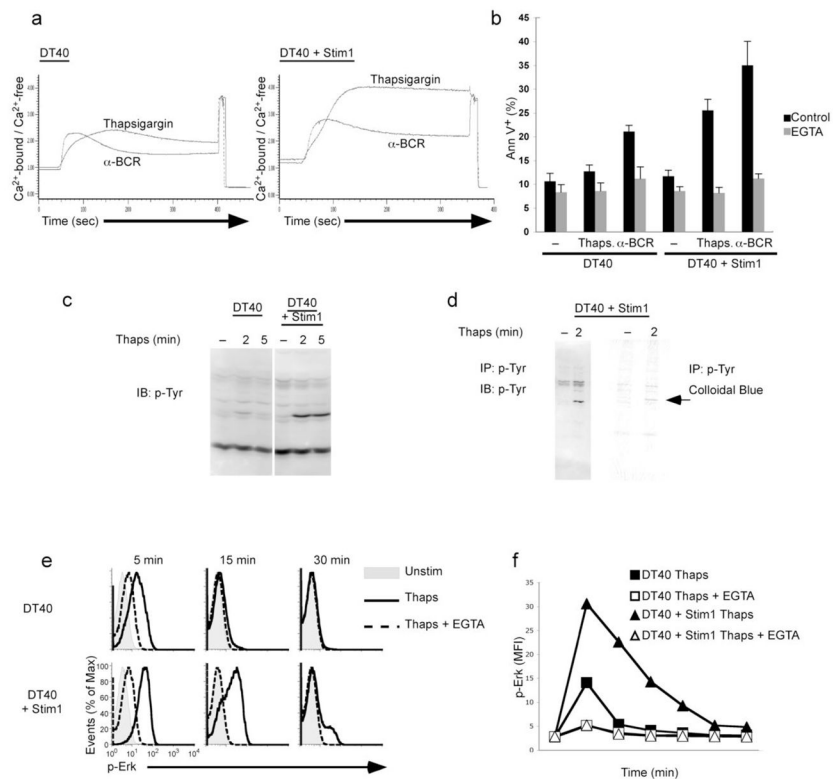
**Figure 1. Sensitization of B cells to antigen-induced apoptosis correlates with $Ca^{2+}$- dependent Erk activation**

**(a)** Intracellular $Ca^{2+}$ measurements following stimulation with 1 μM thapsigargin or the anti-BCR antibody M4. Stimulation was terminated by lysis (maximum $Ca^{2+}$-bound emissions), followed by $Ca^{2+}$ chelation with EGTA (maximum $Ca^{2+}$-free emissions). **(b)** Cells were stimulated for 8 h, and analyzed for surface Annexin V staining. Error bars: s.e.m. ($n$ = 5 experiments) **(c)** Thapsigargin-stimulated cells were lysed and analyzed by immunoblotting with the phosphotyrosine antibodies 4G10 and RC20. **(d)** Phosphotyrosine-containing proteins were immunoprecipitated with the 4G10 antibody from lysates of thapsigargin-stimulated Stim1-overexpressing DT40 cells. Immunoprecipitates were resolved by SDS-PAGE, analyzed by immunoblot (left) or stained with colloidal blue (right). The indicated band was excised and identified as Erk2 by mass spectrometry. This experiment was performed once. **(e)** Thapsigargin-stimulated cells were analyzed by flow cytometry for phospho-Erk (pErk) intensity. **(f)** Graph of the mean fluorescence intensity (MFI) for pErk over time in 1E. The data in panels a, c, e and f are representative of at least 5 experiments each.
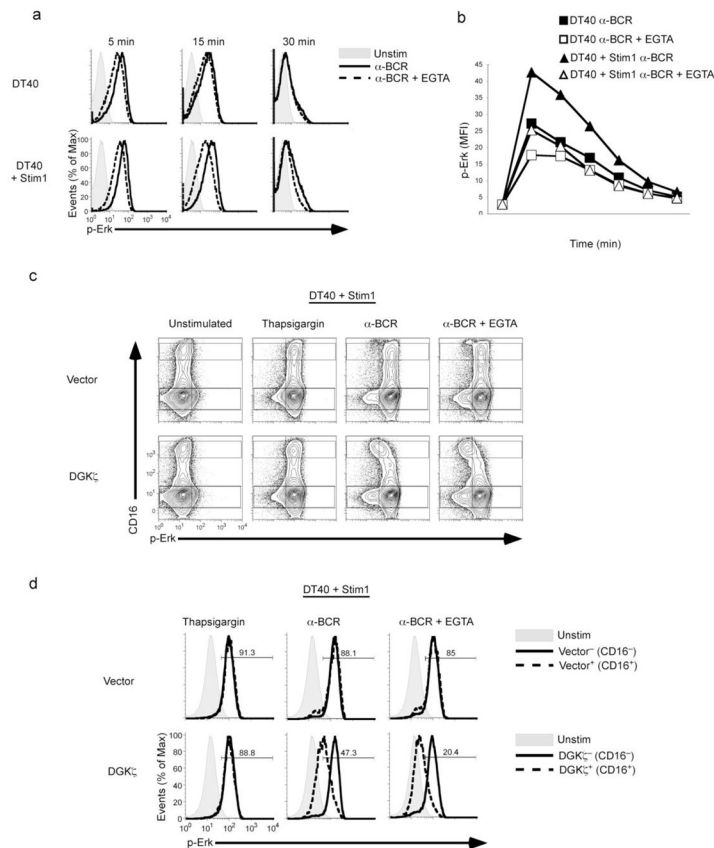
**Figure 2. BCR stimulation activates Erk via two distinct pathways primarily activated by either Ca$^{2+}$ or DAG**

**(a)** Anti-BCR-stimulated cells were analyzed by flow cytometry for phospho-Erk (pErk) intensity. **(b)** The mean fluorescence intensity (MFI) for pErk over time was graphed. Data are representative of at least five independent experiments. **(c,d)** DT40 cells stably overexpressing Stim1 were transiently transfected with CD16 and either vector or DGKζ constructs. The cells were harvested 16–20 h post-transfection, stimulated for 5 min with 1 μM thapsigargin or anti-BCR and the abundance of pErk was analyzed by flow cytometry. Surface CD16 was stained along with pErk, and served as a marker to distinguish transfected from untransfected populations within the same sample (gated populations shown in **c**). Histograms represent pErk response in each population as indicated, and the numbers indicate the percent pErk^{+} cells in the corresponding CD16^{+} population **(d).** The data in panels a-d are representative of at least 3 experiments.
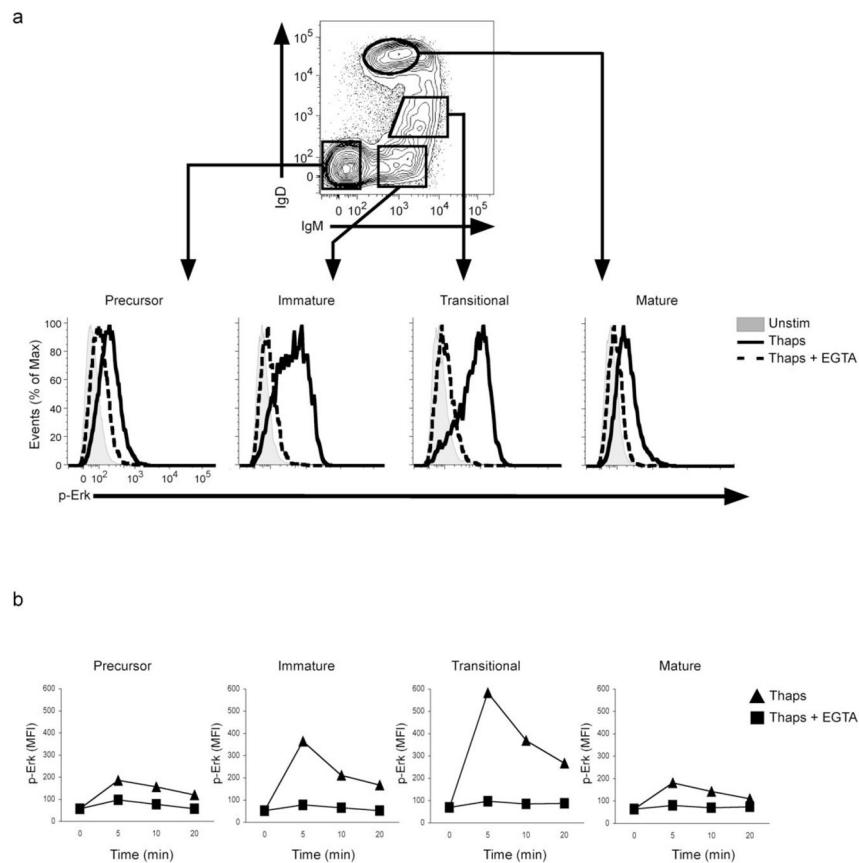
**Figure 3. Ca$^{2+}$-dependent Erk activation occurs selectively at stages of negative selection in primary bone marrow B cells**

**(a)** Bone marrow cells from WT C57BL/6 mice were stimulated with thapsigargin, fixed, permeabilized and stained for pErk along with cell surface markers. B220$^+$ cells were gated in 4 subsets are defined as B220$^+$IgM$^-$IgD$^-$ (precursors), B220$^+$IgM$^+$IgD$^-$ (immature), B220$^+$IgM$^{hi}$IgD$^{int}$ (transitional), B220$^+$IgM$^{lo}$IgD$^+$ (mature recirculating) as shown in upper dot plot. The pErk response was analyzed for each subset. **(b)** Graphs of the mean fluorescence intensity of the pErk response for each subset over time. The data are representative of at least 3 experiments.
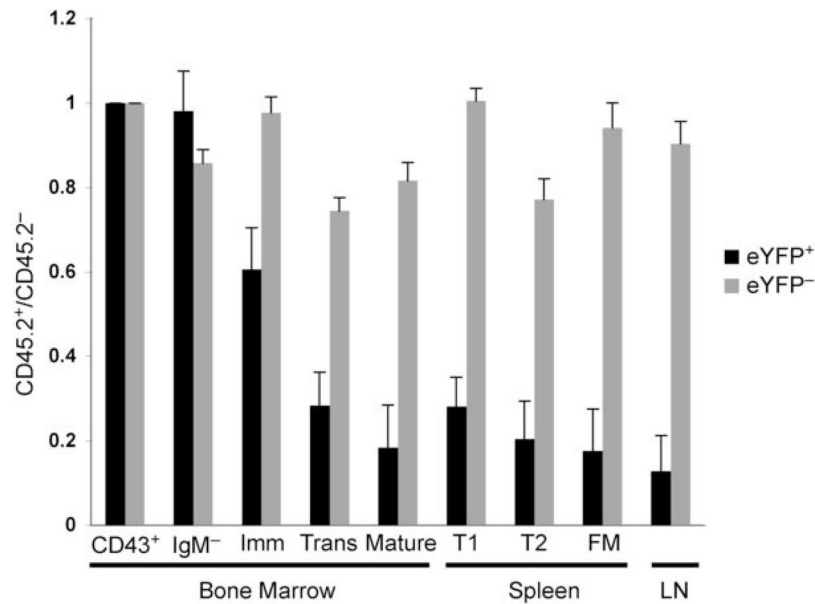
**Figure 4. Stim1 overexpression confers a competitive disadvantage to developing B cells**
CD45.1[+/+] or CD45.1[+]CD45.2[+] purified bone marrow hematopoietic stem cells were infected with retroviruses carrying eYFP or eYFP-Stim1, respectively. Infected cells were mixed at a 1:1 ratio and injected with uninfected carrier bone marrow of the same genotype into lethally irradiated CD45.2[+/+] hosts. Host mice were analyzed 8–10 weeks post-injection. Bone marrow, splenic and lymph node cells were harvested, stained for various cell surface markers and analyzed by flow cytometry. The ratios of CD45.1[+]CD45.2[+] to CD45.1[+/+] cells were calculated for the infected (eYFP[+]) or uninfected (eYFP[−]) populations at various stages in B cell development (corresponding to the eYFP-Stim1^{+} to eYFP[+] ratio in the infected population). Data represents one of three cohorts of reconstituted mice. Error bars: s.e.m. for this cohort ($n = 5$ mice).
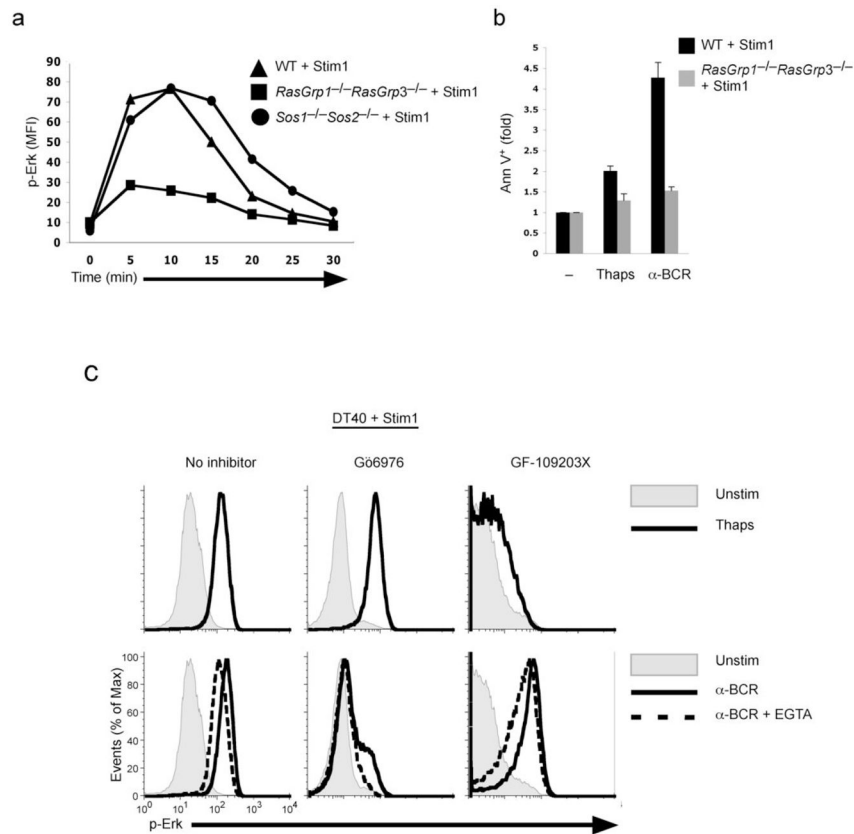
**Figure 5. Activation of Erk downstream of Ca$^{2+}$ requires RasGrp**

**(a)** WT, *Rasgrp1$^{-/-}$ Rasgrp3$^{-/-}$*, or *Sos1$^{-/-}$Sos2$^{-/-}$* DT40 cells were transiently transfected with eYFP-Stim1. Cells were stimulated with thapsigargin as indicated, fixed, permeabilized and stained for pErk. Results show pErk intensity in the eYFP-Stim1-expressing population. Data are representative of two independent experiments. **(b)** Cells stably overexpressing Stim1were stimulated for 8 h, and analyzed for surface Annexin V. Results are expressed as fold-increase in Annexin V$^+$ cells relative to unstimulated cells. Error bars: s.e.m. ($n = 5$ experiments). **(c)** WT DT40 cells stably over-expressing Stim1 were treated with the indicated PKC inhibitors for 5 min, stimulated with thapsigargin or anti-BCR antibody for 5 min, and analyzed for pErk intensity. Data are representative of at least two independent experiments.
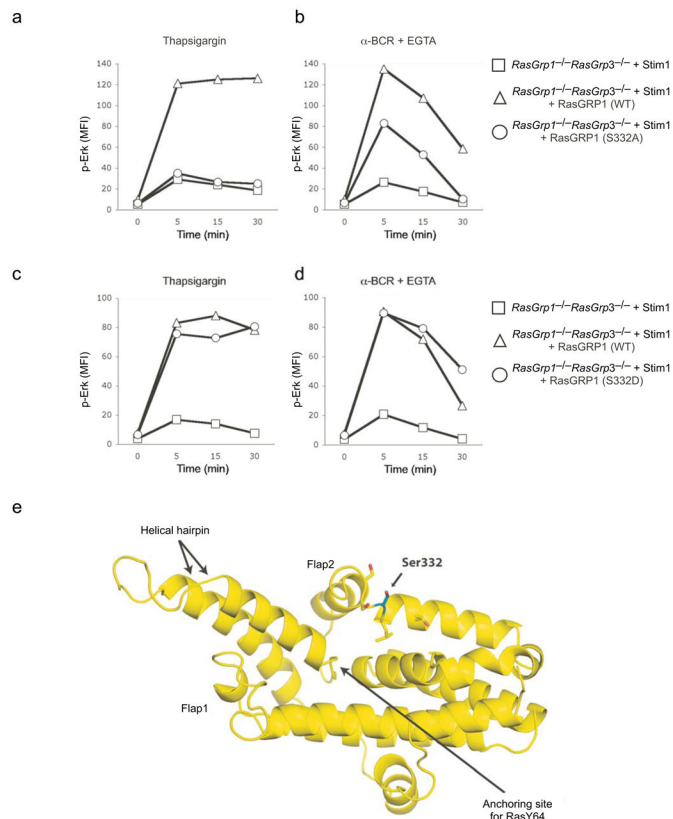
**Figure 6. Phosphorylation of S332 RasGRP1 is required for RasGRP1 to restore Ca$^{2+}$-dependent Erk activation in RasGRP-deficient cells**

RasGRP-deficient Stim1-overexpressing cells were transiently tranfected with WT or mutant Myc-tagged human RasGRP1 constructs. The cells were stimulated as indicated and the pErk response analyzed. Plots show MFI of pErk over time following stimulation. **(a,b)** Effect of S332A mutation on the pErk response induced by thapsigargin **(a)** or by BCR crosslinking in the presence of EGTA **(b)** Data are representative of at least four independent experiments. **(c,d)** Effect of S332D mutation on the pErk response induced by thapsigargin **(c)** or by BCR crosslinking in the presence of EGTA **(d)**. Data are representative of two independent experiments **(e)** The three-dimensional structure of the Cdc25 domain of mouse RasGRP1 was modeled using the ModWeb server and the template mouse RasGRF1 (pdb 2IJE). The potential phosphorylation site at serine 332 (blue sticks) was found to be in flap2 abutting the helical hairpin. Residues within 3.2 Å of S332 are shown in stick representation.
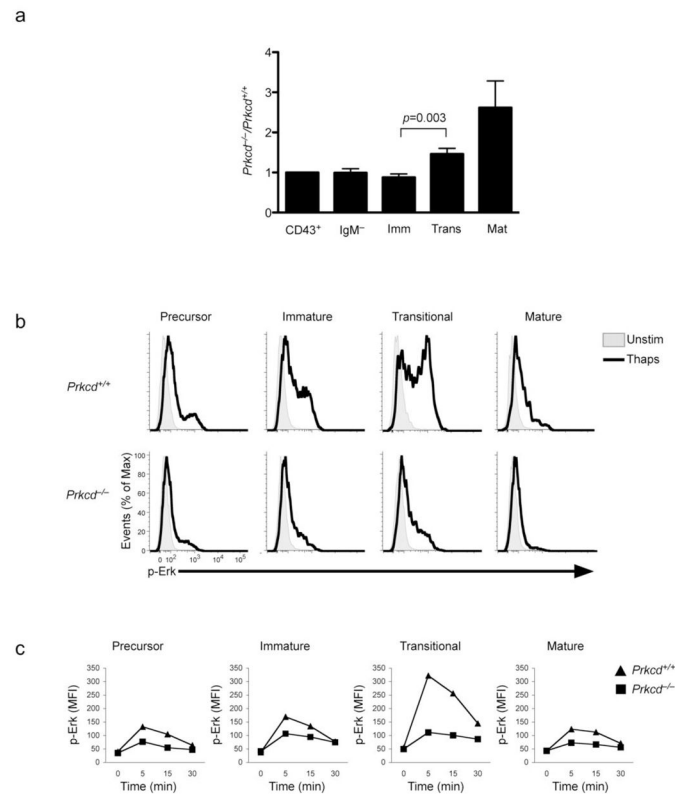
**Figure 7. PKCδ is required for Ca$^{2+}$-dependent Erk activation in developing bone marrow cells**
**(a)** *Prkdc*$^{-/-}$ and WT bone marrow cells bearing different CD45 congenic markers were mixed at a 1:1 ratio and injected into lethally irradiated hosts. Mice were analyzed 6–8 weeks post injection. Graph shows the ratio of *Prkdc*$^{-/-}$ to WT cells throughout B cell development. Data represents one of two cohorts of mice. Error bars: s.e.m. ($n$ = 8 mice) **(b)** *Prkcd*$^{-/-}$ and WT control bone marrow cells were stimulated with thapsigargin as indicated. The pErk response was analyzed by flow cytometry. **(c)** Fold-induction of the MFI of pErk in 3A in each bone marrow subset with respect to resting cells. Data are representative of at least four independent experiments.
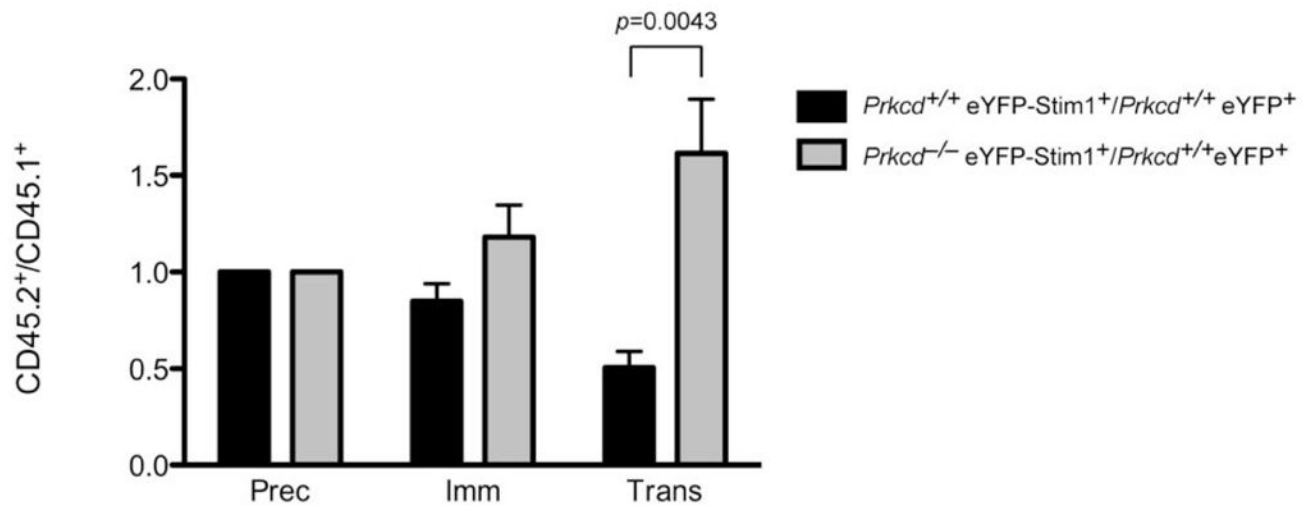
**Figure 8. PKCδ is required for Stim1-mediated sensitization of bone marrow B cells to negative selection**

CD45.1$^{+/+}$ HSCs were infected with retroviruses carrying eYFP and mixed 1:1 with eYFP-Stim1-infected CD45.2$^{+/+}$ HSCs from either WT or $Prkdc^{-/-}$ mice. The cells were injected with uninfected carrier bone marrow of the same genotype into lethally irradiated CD45.1$^{+/+}$ CD45.2$^{+/+}$ hosts. Host mice were analyzed 8–10 weeks post-injection as described in Fig. 4. Data represents one of three cohorts of mice. Error bars: s.e.m. ($n = 11$ mice reconstituted with eYFP-Stim1-infected $Prkdc^{-/-}$ cells and $n = 8$ mice reconstituted with eYFP-Stim1-infected WT cells).